

Periodic Trends in Monoatomic Chemisorbate Bonding on Platinum-Group and Other Noble-Metal Electrodes As Probed by Surface-Enhanced Raman Spectroscopy

Melissa F. Mrozek and Michael J. Weaver*

Contribution from the Department of Chemistry, Purdue University, West Lafayette, Indiana 47907-1393

Received July 26, 1999

Abstract: Metal–adsorbate vibrations evaluated by surface-enhanced Raman spectroscopy (SERS) are reported for chloride, bromide, and sulfide on four Pt-group electrode materials (platinum, palladium, rhodium, and iridium) in comparison with Group IB surfaces (copper, silver, and gold) to ascertain periodic trends in monoatomic chemisorbate bonding at electrochemical interfaces in comparison with theoretical predictions and related vibrational behavior at metal–vacuum interfaces. The measurements utilize our recently developed strategies for preparing ultrathin yet pinhole-free Pt-group films on gold, yielding near-optimal SER spectra essentially free from substrate interferences. The metal–adsorbate stretching frequencies, ν_{M-X} , and derived force constants, f_{M-X} , for all three chemisorbates display the same periodic trends, the f_{M-X} values decreasing from left to right across the 4d and 5d series, increasing from 4d to 5d within a given group. While the ν_{M-X} values for bromide and especially chloride on silver and gold blueshift significantly with increasing electrode potential, symptomatic of partial ionic bonding, this potential dependence is smaller on the Pt-group electrodes, indicative of more covalent bonding, i.e., with greater charge transfer. The f_{M-X} values for chloride increase more sharply toward the left of the 4d and 5d series than for bromide or sulfide, also indicative of metal-dependent covalency. The observed metal-dependent f_{M-X} values can be understood at least qualitatively on the basis of simplified theoretical treatments invoking d-band occupancy, as enunciated earlier to describe surface bonding for oxygen and related adsorbates. The present electrode metal-dependent bonding trends, however, are not dissimilar to those evident from the Raman spectra of symmetric mononuclear metal halide complexes. Related periodic trends are also briefly considered for corresponding vibrational data for chemisorbed carbon monoxide on Pt-group electrodes.

Introduction

Elucidating the nature of chemisorbate–surface bonding at different metal electrodes is a topic having central fundamental significance in electrochemistry, as are such issues for these systems along with analogous metal–vacuum interfaces to surface science in general. While vibrational methods have been used extensively for characterizing surface bonding at in situ electrochemical as well as metal–vacuum interfaces, the infrared reflection–absorption (IRAS) and (to a lesser extent) infrared-visible sum-frequency generation (SFG) spectroscopies¹ employed for scrutinizing metal-dependent chemisorption are largely limited to intramolecular adsorbate vibrations, since the surface–chemisorbate modes usually lie at frequencies below the accessible range of these methods. The latter vibrational modes, however, are of obvious importance for elucidating the nature of the surface chemical bond. Although electron energy loss spectroscopy (EELS) has been used extensively to examine metal–adsorbate vibrational modes, the technique is inherently limited to ultrahigh vacuum (UHV) interfaces. As a consequence, there is a paucity of information regarding surface bonding in electrochemical systems.

(1) For recent reviews of IRAS and SFG applied to electrochemical systems, see: (a) Weaver, M. J.; Zou, S. *Spectroscopy for Surface Science*. In *Advances in Spectroscopy*; Clark, R. J. H., Hester, R. E., Eds.; Wiley: Chichester, 1998; Vol. 26, Chapter 5. (b) Tadjeddine, A.; Peremans, A. *Spectroscopy for Surface Science*. In *Advances in Spectroscopy*; Clark, R. J. H., Hester, R. E., Eds.; Wiley: Chichester, 1998; Vol. 26, Chapter 4.

Surface-enhanced Raman spectroscopy (SERS), with its wide accessible frequency range as well as unique sensitivity, can readily detect metal–chemisorbate as well as most intramolecular adsorbate vibrational modes in electrochemical and other ambient environments. Indeed, it has been widely used for this purpose with the coinage-metal substrates (copper, silver, and gold) that display intrinsic SERS activity with visible laser excitation when suitably roughened.^{1a,2} This laboratory has long been interested in strategies for extending the applicability of SERS to a wider range of surface materials,^{3–5} especially to Pt-group transition metals⁵ in view of their catalytic importance.

(2) Insightful reviews describing fundamental electrochemical applications of SERS include the following: (a) Pettinger, B. In *Adsorption of Molecules at Electrodes*; Lipkowsky, J., Ross, P. N., Eds.; VCH Publishers: New York, 1992; Chapter 6. (b) Pemberton, J. E. In *Electrochemical Interfaces—Modern Techniques for in-situ Interface Characterization*; Abruna, H. D., Ed.; VCH Publishers: New York, 1991; Chapter 5. (c) Hester, R. E. In *Comprehensive Chemical Kinetics*; Compton, R. G., Hammett, A., Eds.; Elsevier: Amsterdam, 1989; Vol. 29, Chapter 2. (d) Brandt, E.-S.; Cotton, T. M. In *Investigations of Surfaces and Interfaces, Part B*; Rossiter, B. W., Baetzold, R. C., Eds.; Physical Methods of Chemistry Series, 2nd ed.; Wiley: New York, 1993; Vol. 9B, Chapter 8. (e) Brolo, A. G.; Irish, D. E.; Smith, B. D. *J. Mol. Struct.* **1997**, 405, 29.

(3) For a recent overview see: Weaver, M. J.; Zou, S.; Chan, H. Y. H. *Anal. Chem.* **2000**, 72, 44A.

(4) (a) Desilvestro, J.; Corrigan, D. A.; Weaver, M. J. *J. Phys. Chem.* **1986**, 90, 6408. (b) Zou, S.; Weaver, M. J. *J. Phys. Chem. B* **1999**, 103, 2323. (c) Leung, L.-W. H.; Weaver, M. J. *J. Electroanal. Chem.* **1987**, 217, 367. (d) Leung, L.-W. H.; Gosztola, D.; Weaver, M. J. *Langmuir* **1987**, 3, 45.

(5) (a) Leung, L.-W. H.; Weaver, M. J. *J. Am. Chem. Soc.* **1987**, 109, 5113. (b) Leung, L.-W. H.; Weaver, M. J. *Langmuir* **1988**, 4, 1076.

The most versatile tactic involves the electrodeposition of ultrathin (2–5 monolayer, ML) transition-metal films onto a SERS-active gold substrate. Such films, which impart near-optimal SERS activity to adsorbates on the overlayer metal, have been employed extensively in our laboratory to examine chemisorption and heterogeneous catalysis on transition metals in ambient-pressure gaseous environments at elevated temperatures⁶ as well as in electrochemical systems.^{5,7}

A factor restricting especially electrochemical applications of the transition-metal overlayers has been the common presence of exposed residual gold sites, yielding spectral and electrochemical interferences from the substrate. Recently, however, Zou et al. have devised modified constant-current electrodeposition procedures that yield ultrathin Pt-group metal overlayers displaying optimal SERS properties that are essentially *pinhole-free*, and thereby devoid of substrate interferences.⁸ While thicker films yield progressively weaker SERS signals, a significant and eventually dominant contribution to the Raman enhancement has been shown to emanate from the transition-metal overlayer itself.⁹ These developments offer the intriguing prospect of examining vibrational spectra for a much wider range of adsorbates at transition-metal electrochemical interfaces, including species that bind also to gold electrodes. Indeed, we have recently examined the chemisorption of benzene and monosubstituted benzenes, along with thiocyanate, on Pt-group metal electrodes by this means;¹⁰ the rich SER spectra obtained for the former organic systems, in particular, provide detailed information on the molecular orientation and surface binding.^{10a,b}

Especially simple, and thereby instructive, monoatomic chemisorbate systems to examine with regard to surface binding are the halogens, oxygen, and sulfur. Oxygen adsorption at Pt-group electrodes, triggered most readily by water oxidation, is complicated by surface oxide formation (i.e., oxygen penetration into the metal lattice). Described elsewhere are SER studies of the latter in electrochemical and gaseous environments.¹² However, monoatomic halogen and sulfur adsorbates are readily formed at metal–solution interfaces from the solute anions. Halides constitute archetypical monoatomic chemisorbates in electrochemistry, exhibiting strongly electrode potential-dependent binding. We have previously examined potential-dependent metal–halide stretching frequencies, ν_{M-X} , by means of SERS on gold electrodes, and noted differences in the surface bonding in comparison with silver electrodes.¹¹ Armed with our improved metal overlayer procedures, we have now been able to acquire related potential-dependent SER spectra for chloride and bromide adsorbed on four Pt-group metals: platinum, palladium, iridium, and rhodium. The salient results are described herein. Together with data for the adjoining Group IB “coinage” metals gold, silver, and copper, the findings enable periodic trends in the surface bonding to be explored in a fashion that is unprecedented for electrochemical interfaces. While the ν_{M-X} frequencies provide only partial information on metal–

adsorbate bond energies, E_{ad} , the latter quantities are elusive for electrochemical systems; at least periodic trends in E_{ad} should be discernible from the relative ν_{M-X} values. Also presented herein are SER spectra for sulfide adsorption on the four Pt-group electrodes. While the spectral behavior of this chemisorbate is complicated by potential-dependent protonation equilibria and electrooxidation to polysulfur species,^{7b,13} the tenacious metal–sulfur binding also yields periodic trends for comparison with halogen bonding, not only at the electrochemical interfaces but also for related metal–UHV systems examined by EELS.

Experimental Section

Most details of the SERS experimental arrangement are given in previous reports, especially ref 7b. The Raman excitation was at 647.1 nm, with ca. 30 mW power focused to a ca. 1 mm spot on the electrode surface. Scattered light was collected into a SPEX Triplemate spectrometer equipped with a CCD detector. The gold electrode substrates were 2–4 mm disks sheathed in Teflon. They were roughened so to engender stable SERS activity prior to each experiment by means of oxidation–reduction cycles in 0.1 M KCl, as outlined in ref 14. The subsequent transition-metal electrodeposition onto the SERS-active gold followed the procedures outlined in ref 8. Typically, 3–5 monolayers were deposited, using either an acidic medium, 0.1 M HClO₄ (for Pd and Rh), or a phosphate buffer solution, 0.7 M Na₂HPO₄ (for Pt and Ir). The overlayer films were checked for pinhole-free uniformity by cycle voltammetry in 0.1 M HClO₄.^{8a} Double-distilled (70%) perchloric acid and sodium perchlorate were from GFS Chemicals, sodium hydroxide from Baker, and sodium phosphate from Sigma. Solutions were prepared using ultrapure water from a MilliQ Plus system (Millipore). All measurements were performed at room temperature (23 ± 1 °C), and electrode potentials were measured and are reported versus the saturated calomel electrode (SCE).

Results

Halide Chemisorption. The basic measurement protocol followed here was to acquire SER spectra on all four Pt-group surfaces for both chloride and bromide over potential regions, typically ca. –0.2 to 0.5 V, over which cyclic voltammetry indicated an absence of surface reduction or oxidation processes, and where the changes in Raman signals were largely reversible upon potential alteration. An acidic electrolyte, 0.1 M HClO₄, was chosen so to enable positive potentials to be accessed, at which strong halide chemisorption occurs. The halide concentration was typically 10 mM, although varying this over the range 5–100 mM yielded similar results.

Representative potential-dependent sets of SER spectra for chloride and bromide on the four Pt-group electrodes, as indicated, are shown in Figures 1 and 2, respectively. Clearly evident in each case is a Raman band peaked at 270–320 cm^{–1} for chloride and 185–200 cm^{–1} for bromide. By comparison with the frequencies for related systems in electrochemical and vacuum environments (vide infra),¹¹ the bands can be assigned with confidence to metal surface–halogen stretching vibrations, ν_{M-X} . Corresponding measurements for adsorbed iodide yielded a weak feature at 100–150 cm^{–1}, having the same assignment; however, the low intensity of this mode combined with substantial interference from the Rayleigh scattering “tail” thwarted quantitative measurements with our spectrometer. The metal–chloride band intensity is seen to decrease somewhat toward lower potentials, especially on palladium and platinum (Figure 1), approximately consistent with diminutions in adsorbate coverage as deduced from radiotracer, rotating-disk, and other measurements.¹⁵ (An approximate correlation was

(6) For example: (a) Williams, C. T.; Takoudis, C. G.; Weaver, M. J. *J. Phys. Chem. B* **1998**, *102*, 406. (b) Tolia, A.; Williams, C. T.; Takoudis, C. G.; Weaver, M. J. *J. Phys. Chem.* **1995**, *99*, 4599.

(7) (a) Zhang, Y.; Gao, X.; Weaver, M. J. *J. Phys. Chem.* **1993**, *97*, 8656. (b) Gao, X.; Zhang, Y.; Weaver, M. J. *Langmuir* **1992**, *8*, 668.

(8) (a) Zou, S.; Weaver, M. J. *Anal. Chem.* **1998**, *70*, 2387. (b) Zou, S.; Gómez, R.; Weaver, M. J. *Langmuir* **1997**, *13*, 6713.

(9) Zou, S.; Weaver, M. J.; Li, X. Q.; Ren, B.; Tian, Z. Q. *J. Phys. Chem. B* **1999**, *103*, 4218.

(10) (a) Zou, S.; Williams, C. T.; Chen, E. K.-Y.; Weaver, M. J. *J. Am. Chem. Soc.* **1998**, *120*, 3811. (b) Zou, S.; Williams, C. T.; Chen, E. K.-Y.; Weaver, M. J. *J. Phys. Chem. B* **1998**, *102*, 9039, 9743. (c) Luo, H.; Weaver, M. J. *Langmuir*. In press.

(11) Gao, P.; Weaver, M. J. *J. Phys. Chem.* **1986**, *90*, 4057.

(12) (a) Zou, S.; Chan, H. Y. H.; Weaver, M. J. *Langmuir*. In press. (b) Chan, H. Y. H.; Zou, S.; Weaver, M. J. *J. Phys. Chem. B*. In press.

(13) Gao, X.; Zhang, Y.; Weaver, M. J. *J. Phys. Chem.* **1992**, *96*, 4156.

(14) Gao, P.; Gosztola, D.; Leung, L.-W. H.; Weaver, M. J. *J. Electroanal. Chem.* **1987**, *233*, 211.

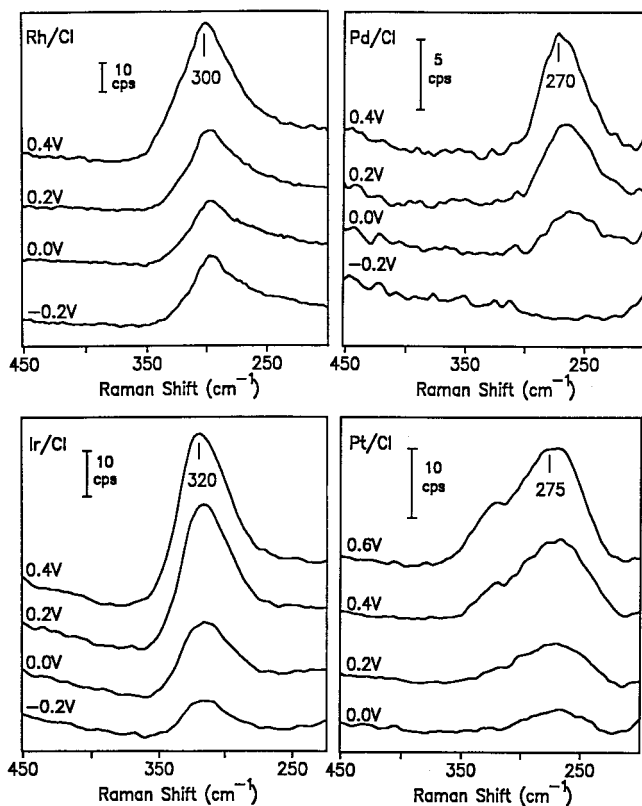


Figure 1. Electrode potential-dependent SER spectra for chloride adsorbed on Rh, Pd, Ir, and Pt films on gold from aqueous 10 mM NaCl in 0.1 M HClO₄.

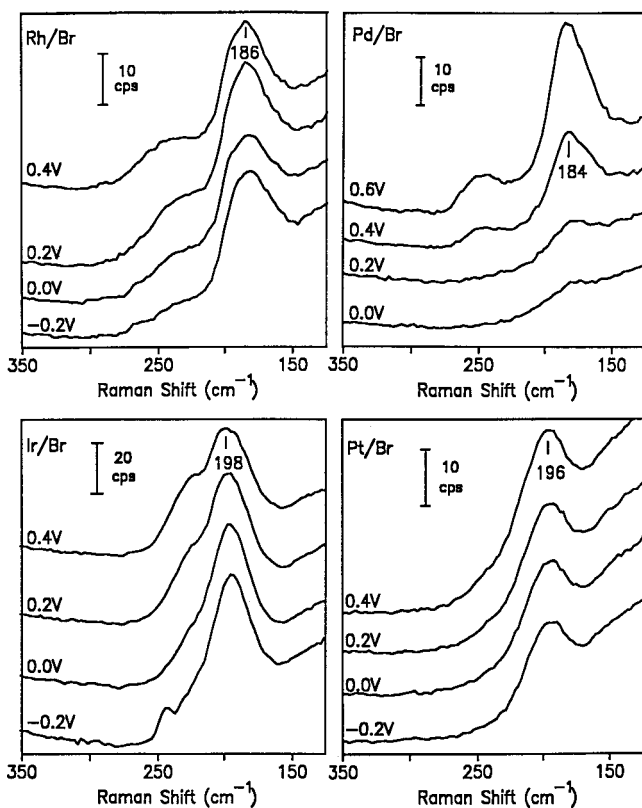


Figure 2. Electrode potential-dependent SER spectra for bromide adsorbed on Rh, Pd, Ir, and Pt films on gold from aqueous 10 mM NaBr in 0.1 M HClO₄.

found earlier between the reversible potential-dependent SERS intensities and the coverages of halide and pseudohalide

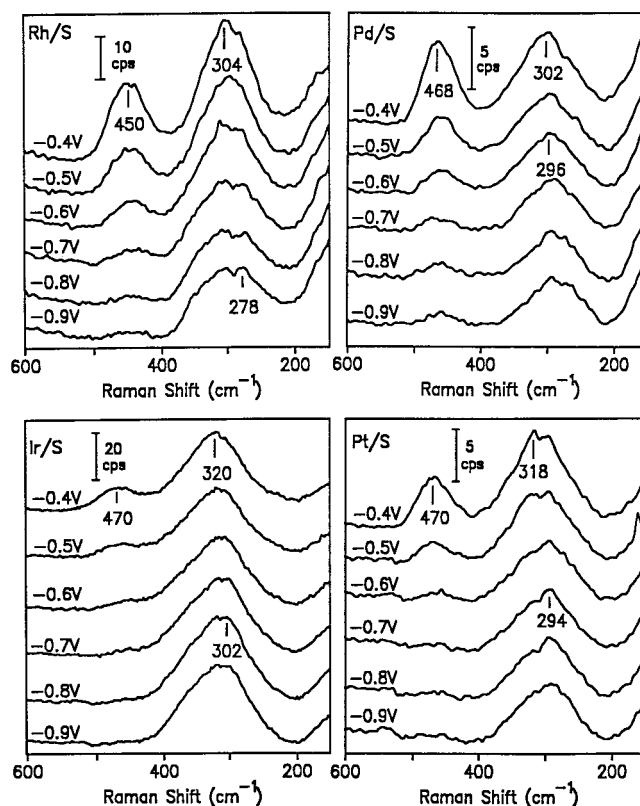


Figure 3. Electrode potential-dependent SER spectra for sulfide adsorbed on Rh, Pd, Ir, and Pt films on gold from aqueous 10 mM Na₂S in 0.1 M NaClO₄ + 1 mM NaOH.

adsorbates on silver electrodes.¹⁶) The effect is less evident for bromide except on palladium, in harmony with the stronger electrochemical adsorption usually observed in comparison with chloride. Roughly symmetric ν_{M-X} band shapes are obtained in most cases, although higher-frequency shoulders are evident for the Pt-Cl and Ir-Br systems at the most positive potentials.

Aside from the peak frequencies, ν_{M-X}^P , themselves, their potential dependence is of interest.¹¹ While complicated somewhat by partial halide desorption toward negative potentials, small yet nonzero ($d\nu_{M-X}^P/dE$) values are discernible. Approximate values are the following: Pd-Cl, 20 cm⁻¹ V⁻¹; Rh-Cl, 15 cm⁻¹ V⁻¹; Ir-Cl, 10 cm⁻¹ V⁻¹; and Rh-Br, Ir-Br, and Pt-Br, 5 cm⁻¹ V⁻¹. Significantly, however, these slopes for chloride adsorption are much smaller than those obtained on gold and silver (vide infra).¹¹

Similar potential-dependent SER spectra were also obtained for adsorbed sulfide. Figure 3 shows such data obtained again for the four Pt-group surfaces, as indicated, in 0.1 M NaClO₄ + 1 mM NaOH, containing 10 mM Na₂S. The alkaline electrolyte was chosen not only to avoid H₂S formation, but also to minimize complications from sulfide protonation in the chemisorbed state. The latter effect has been shown to yield an SH adsorbate at more negative potentials on gold, distinguished by a 30–40 cm⁻¹ lower metal-sulfur stretching frequency.^{7b} The SER spectra in Figure 3 show a broad band around 280–320 cm⁻¹ on each metal, accompanied by a higher-frequency feature at 450–470 cm⁻¹ at the least negative potentials. By comparison

(15) For example, see: (a) Horanyi, G.; Rizmayer, E. M. *Electrochim. Acta* **1985**, *30*, 923. (b) Horanyi, G.; Rizmayer, E. M. *J. Electroanal. Chem.* **1986**, *198*, 379. (c) Bockris, J. O'M.; Gamboa-Aldeco, M.; Szklarczyk, M. *J. Electroanal. Chem.* **1992**, *339*, 355. (d) Gasteiger, H. A.; Markovic, N. M.; Ross, P. N., Jr. *Langmuir* **1996**, *12*, 1414.

(16) Weaver, M. J.; Hupp, J. T.; Barz, F.; Gordon, J. G., II; Philpott, M. R. *J. Electroanal. Chem.* **1984**, *160*, 321.

Table 1. Raman Frequencies and Derived Force Constants for Chloride, Bromide, and Sulfide Adsorbed on Various Electrode Surfaces

vibration	ν_{M-X}^a (cm^{-1})	$10^5 f_{M-X}^b$ (dyn cm^{-1})	ν_{M-X}^a (cm^{-1})	$10^5 f_{M-X}^b$ (dyn cm^{-1})	ν_{M-X}^a (cm^{-1})	$10^5 f_{M-X}^b$ (dyn cm^{-1})
M-Cl					Cu ^c	
					290	1.76
					Ag ^d	
M-Cl	Rh	300	1.88	Pd	270	1.52
M-Br		186	1.63		243	1.23
M-S		304	1.75		165	1.29
					Au ^d	
M-Cl	Ir	320	2.14	Pt	265	1.50
M-Br		198	1.85		185	1.61
M-S		320	1.94		304 ^e	1.75

^a Measured peak frequency for metal–adsorbate stretching vibration.

^b Derived force constant for metal–adsorbate stretch, from eq 1 (see text). ^c From ref 17. ^d At 0.2 V vs SCE from ref 11. ^e At -0.35 V vs SCE from ref 7b. All other vibrational frequencies and derived force constants from this work. Values of ν_{M-X} for halides and sulfide at 0.2–0.4 and -0.4 V vs SCE, respectively.

with earlier data on gold,^{7b} the former feature can be ascribed with confidence to the metal–sulfur stretching vibration, ν_{M-S} . While the peak frequency of this mode, ν_{M-S}^P , appears to redshift significantly (by ca. 15 cm^{-1}) toward lower potentials, at least the spectra on Rh–S suggest that this shift arises from varying contributions from a pair of overlapping bands. It is therefore reasonable to ascribe this apparent ν_{M-S}^P-E dependence to the occurrence of adsorbate protonation at the lower potentials (cf. ref 7b). The ca. 450 cm^{-1} band present at the highest potentials can be ascribed to the S–S stretch associated with adsorbed polysulfur, formed by the onset of sulfide electrooxidation, again with reference to the earlier detailed SERS study of sulfide on gold electrodes.^{7b} Additional bands at 220 and 150 cm^{-1} appear above ca. -0.2 V, also diagnostic of polysulfide formation.^{7b}

Of particular interest here is the dependence of the metal–adsorbate stretching vibrations on the metal surface. To this end, Table 1 lists values of ν_{M-X}^P and ν_{M-S}^P for each system studied here. The former values refer to the potential region, 0.2–0.4 V, where the halide coverages should approach saturation, coinciding with higher band intensities. The ν_{M-S} values refer to more negative potentials, -0.4 to -0.6 V, necessitated by the desire to avoid extensive polysulfur formation. Despite these differences, the small observed $d\nu_{M-X}/dE$ values suggest that the precise choice of potential with which to compare the band frequencies for different adsorbates on Pt-group metals is relatively unimportant.

Listed in the right-hand column of Table 1, in periodic fashion alongside the present data for the Pt-group metals, are corresponding vibrational data on copper, silver, and gold, extracted for similar conditions from previous studies in this laboratory.^{7b,11,17} The ν_{M-X}^P values listed for gold and silver refer to 0.2 V vs SCE, chosen so to correspond approximately to the conditions to which the Pt-group data refer. Note that the choice of electrode potential, however, is important at least for the Au–Cl and Ag–Cl systems in view of their significant ($d\nu_{M-X}/dE$) values:¹¹ for Au–Cl, $35 \text{ cm}^{-1} \text{ V}^{-1}$; Ag–Cl, $20 \text{ cm}^{-1} \text{ V}^{-1}$; also for Au–Br, $8 \text{ cm}^{-1} \text{ V}^{-1}$; Ag–Br, $\sim 15 \text{ cm}^{-1} \text{ V}^{-1}$.

In addition to the experimental metal–adsorbate frequencies, values are given alongside in Table 1 of the corresponding force constants, f_{M-X} , as given by the usual formula (cf. ref 11):

$$f_{M-X} = 4\pi^2(\nu_{M-X}^P)^2 c^2 \mu \quad (1)$$

where c is the velocity of light and μ is the reduced mass of the vibrating bond. The last quantity is taken for simplicity as the adsorbate mass. While this procedure is only approximate in view of anticipated coupling between metal–adsorbate and metal–metal vibrations,¹⁹ we are primarily concerned here only with variations in f_{M-X} for a given adsorbate on different metals. While the peak frequency of the Raman bands is the most intuitively reasonable parameter for our purposes, the breadth of these features suggests a degree of surface inhomogeneity, perhaps together with multiple binding-site geometries on the polycrystalline surfaces necessarily employed here. Multifold surface coordination should always be preferred for such monoatomic adsorbates,²⁰ although a distribution of geometries might be expected at high coverages. The bandwidths may well reflect such distributions since metal–adsorbate frequencies should increase as the surface bond order decreases.²¹ Again, however, the metal-dependent trends in the apparent f_{M-X} values, of primary concern here, should be insensitive to such details.

Discussion

Careful inspection of Table 1 reveals intriguing periodic trends in the metal–adsorbate frequencies and derived force constants for the seven Pt-group and Group IB metals amenable to comparative examination by SERS. Monotonic decreases in the force constants are observed as one progresses from left to right across a periodic series. This finding suggests a correlation with the electron filling of the metal d band (vide infra), since this property progressively increases across the series. The trend is consistent for M–Cl, M–Br, and M–S force constants across the 4d and 5d series, where uniformly $f_{Rh-X} > f_{Pd-X} > f_{Ag-X}$ and $f_{Ir-X} > f_{Pt-X} > f_{Au-X}$. In addition, the force constants are sensitive to whether the metal valence electrons are 3d, 4d, or 5d. Inspection of Table 1 reveals that f_{M-X} increases down a periodic group from the 4d to the 5d metal surfaces: for each of the three monoatomic adsorbates, $f_{Rh-X} < f_{Ir-X}$, $f_{Pd-X} < f_{Pt-X}$, and $f_{Ag-X} < f_{Au-X}$. A nonmonotonic trend, however, is seen for Group IB metals in that the metal–chloride force constants increase in the order $4d < 5d < 3d$, such that f_{M-Cl} is largest on copper. However, the latter is consistent with harmonic vibrational frequencies extracted from density functional calculations.²²

The relative force constants for the different adsorbates also vary significantly with the metal surface. For the Group IB (Ag, Au) and the late Group VIII metals (Pd, Pt), $f_{M-Cl} < f_{M-Br} < f_{M-S}$, whereas $f_{M-Cl} > f_{M-Br}$ for Rh and Ir (Table 1). The weaker bonding implied for chloride versus bromide, at least on the Group IB metals, may be connected with a smaller degree of bond covalency for the former adsorbate.¹¹ Favoring this notion are the larger ($d\nu_{M-X}^P/dE$) “Stark-tuning” slopes obtained for chloride relative to bromide adsorption, especially on silver and gold (vide supra).¹¹ This is because the presence of a partly ionic $M^{\delta+}-X^{\delta-}$ bond will provide an electrostatic contribution to the vibrational force constant, enhancing f_{M-X} toward more positive potentials, and hence electrode charges.¹¹ The formation of a more covalent coordinate bond, associated therefore with

(18) (a) Pettinger, B.; Philpott, M. R.; Gordon, J. G., II *J. Phys. Chem.* **1981**, *85*, 2746. (b) Niaura, G.; Malinauskas, A. *Chem. Phys. Lett.* **1993**, *207*, 455.

(19) Moskovits, M. *Chem. Phys. Lett.* **1983**, *98*, 498.

(20) Shustorovich, E. *Surf. Sci. Rep.* **1986**, *6*, 1.

(21) Andersson, S. *Chem. Phys. Lett.* **1978**, *55*, 185.

(22) Ignaczak, A.; Gomes, J. A. N. F. *J. Electroanal. Chem.* **1997**, *420*, 71.

(17) Chan, H. Y. H.; Takoudis, C. G.; Weaver, M. J. *J. Phys. Chem. B* **1999**, *103*, 357.

greater ion discharge upon chemisorption, will be expected on this basis to yield smaller Stark-tuning slopes. The present observation that $(d\nu_{M-X}^P/dE)$ decreases from right to left across the 4d and 5d series, especially for chloride, therefore also suggests that bond covalency is more prevalent on the Group VIII compared with the IB metals. (Essentially complete ion discharge in the Pt/Br system, for example, is consistent with a measured "electrosorption valency" of unity.^{15d}) The greater increases in f_{M-X} for chloride relative to bromide in progressing from right to left in the 4d and 5d series (Table 1) can therefore be attributed at least partly to the effects of enhanced bond covalency.

It is of interest to compare the present experimental trends for electrochemical adsorption with ν_{M-X} data for analogous systems in UHV examined by means of EELS. Although the latter data are sparse, by and large the findings are compatible. For example, monoatomic chlorine chemisorbed on the (111) planes of Pt and Pd yields ν_{M-X} values of 300 and 265 cm^{-1} , respectively,²³ thereby mimicking approximately the present behavior. Metal-sulfur stretches on Rh(111), Rh(100), and Pt(111) also exhibit EELS ν_{M-X} values, 300–325 cm^{-1} ,²⁴ close to the SERS band frequencies on these metals. While the EELS data for neither halogens nor sulfur are sufficiently extensive to discern broader periodic trends, data for atomic oxygen adsorption are compatible with the present observations. Thus metal-oxygen EELS frequencies, ν_{M-O} , tend to lie in the sequence $\text{Pt} \leq \text{Pd} \leq \text{Rh} < \text{Ir}$. Typical literature values are as follows: Pt(111), 460–480 cm^{-1} ,²⁵ Pd(111), 500 cm^{-1} ,²⁶ Rh(111), 520 cm^{-1} ,²⁷ Ir(111), 550 cm^{-1} .²⁸ Indeed, the surface-atomic oxygen bond energies, E_{ad} , known at metal-UHV interfaces exhibit essentially the same periodic trends as observed here for the electrode surface-halogen and -sulfur force constants, again decreasing monotonically from left to right in both the 4d and 5d series. The E_{ad} values follow the order $\text{Rh} > \text{Pd} > \text{Ag}$ and $\text{Ir} > \text{Pt} > \text{Au}$, also $\text{Ir} > \text{Rh}$ and $\text{Cu} > \text{Ag} \sim \text{Au}$,²⁹ thereby following the same metal-dependent f_{M-X} sequences evident for halogens and sulfur in Table 1.

These periodic trends across the 4d and 5d series for monoatomic adsorbates, most commonly discussed in the literature for hydrogen and oxygen, can be accounted for by invoking chemisorption models of adsorbate interaction with the metal d band. One simple chemisorption model entails adsorbate electrons entering "vacancies" in the metal d band, where they are paired with metal d electrons to form a covalent surface bond.^{20,30} For a donor adsorbate, the heat of chemisorption was suggested to be proportional to the metal d-vacancy count. Consequently, a metal surface with more electron vacancies in its d band will be capable of accepting greater

adsorbate charge, thus resulting in a stronger, more covalent metal-adsorbate bond.^{20,30} Thus adsorbate to metal charge transfer decreases on this basis in the order of metal d band filling, $d^8 > d^9 > d^{10}$, such that a more covalent bond is formed at the more electron-deficient surface, in complete accordance with the present experimental findings. The higher force constants observed here on 5d versus 4d metal surfaces may qualitatively be explained by the smaller effective d-orbital population expected for 5d versus corresponding 4d metals.^{31a} (Calculated values are as follows:^{31b} Pt, 8.75; Pd, 8.95; Ir, 7.65; Rh, 8.00.) Accordingly, the 5d metal surface should have greater "d-band vacancies", facilitating adsorbate-metal charge transfer and resulting in more covalent bonding.

A different, yet related, approach to chemisorption invokes the formation of bonding and antibonding adsorbate-metal d states in the interaction between an atomic adsorbate and a metal surface.³² A greater population of antibonding adsorbate-metal d states will result in a weaker surface bond. Accordingly, as the number of d electrons increases for a metal, these antibonding states will become more populated, weakening the bond. Both these approaches to modeling the adsorbate-surface interaction therefore account qualitatively for the present observed periodic trends in metal-halide and metal-sulfur force constants. The dependence upon the number of electrons in the metal d band is a prominent theme in the simplified theoretical analysis of chemisorption energies and related quantities, and on the basis of the present findings is appropriate for describing metal-atomic adsorbate bonding also at charged electrochemical interfaces.

Having deduced the significance of the d-band occupancy to such late transition-metal electrochemical systems, it is nonetheless of interest to compare the present observed trends to vibrational spectra for homologous series of related mononuclear metal-halide complexes. While the bonding description for such systems will necessarily differ from the "band-structure" picture appropriate for metal surfaces, one is reminded of the oft-perceived "localized" nature of metal-adsorbate bonding, for example implicit in comparisons between metal oxide and metal surface-oxygen bond energetics²⁹ and "bond-order conservation" analyses.^{20,30}

Indeed, the Raman symmetric M-X stretching frequencies in MX_6 , $[\text{MX}_6]^{2-}$, and $[\text{MX}_2]^-$ type complexes illustrate similar overall periodic trends to those evident here for electrode-adsorbate vibrations. A steady decrease in the stretching frequencies for MF_6 complexes is found as one progresses from left to right across a periodic series.³³ The $[\text{MCl}_6]^{2-}$ and $[\text{MBr}_6]^{2-}$ complexes display M-X frequencies that are higher for d^8 versus d^9 and 5d versus 4d Pt-group metals.³⁴ Bond strengths for $[\text{MX}_6]^{2-}$ type complexes also exhibit clear periodic trends for 4d and 5d metals ranging from d^4 and d^9 , decreasing from left to right across a series, and increasing from 4d to 5d metals.³⁵ Also similar to the present findings (Table 1), a nonmonotonic trend is evident for Group IB $[\text{MX}_2]^-$ complexes, in that the stretching frequencies increase in the order $4d < 3d < 5d$.³² These findings therefore suggest, perhaps surprisingly,

(23) (a) Zhou, X.-L.; Liu, Z.-M.; Kiss, J.; Sloan, D. W.; White, J. M. *J. Am. Chem. Soc.* **1995**, *117*, 3565. (b) Aarts, J. F. M.; Phelen, K. G. *Surf. Sci.* **1989**, *222*, L853.

(24) (a) Bol, C. W. J.; Friend, C. M.; Xu, X. *Langmuir* **1996**, *12*, 6083. (b) Dubois, L.-H. *J. Chem. Phys.* **1982**, *77*, 5228. (c) Batina, N.; McCarger, J. M.; Salaita, G. N.; Lu, F.; Larguren-Davidson, L.; Lin, C.-H.; Hubbard, A. T. *Langmuir* **1989**, *5*, 123.

(25) Parker, D. H.; Bartram, M. E.; Koel, B. E. *Surf. Sci.* **1989**, *217*, 489.

(26) Ramsier, R. D.; Gao, Q.; Waltenberg, N. H.; Yates, J. T., Jr. *J. Chem. Phys.* **1994**, *100*, 6837.

(27) (a) Root, T. W.; Fisher, G. B.; Schmidt, L. D. *J. Chem. Phys.* **1986**, *85*, 4687. (b) Wagner, F. T.; Moylan, T. E. *Surf. Sci.* **1987**, *191*, 121.

(28) (a) Davis, J. E.; Nolan, P. D.; Karseboom, S. G.; Mullins, C. B. *J. Chem. Phys.* **1997**, *107*, 943. (b) Marinov, T. S.; Kostov, K. L. *Surf. Sci.* **1987**, *185*, 203.

(29) Benziger, J. B. In *Metal-Surface Reaction Energetics*; Shustorovich, E., Ed.; VCH Publishers: New York, 1991; Chapter 2.

(30) Shustorovich, E.; Baetzold, R. C.; Muetterties, E. L. *J. Phys. Chem.* **1983**, *87*, 1100.

(31) (a) Tsai, M. H.; Hass, K. C. *Phys. Rev. B* **1995**, *51*, 14616. (b) Total d-band occupancies extracted from: Papaconstantopoulos, D. A. *Handbook of the Band Structures of Elemental Solids*; Plenum: New York, 1986.

(32) (a) Norskov, J. K. *Prog. Surf. Sci.* **1991**, *38*, 103. (b) Norskov, J. K. *Rep. Prog. Phys.* **1990**, *53*, 1253.

(33) Clark, R. J. H. In *Halogen Chemistry*; Gutmann, V., Ed.; Academic Press: New York, 1967; pp 85–121.

(34) Nakamoto, K. *Infrared and Raman Spectra of Inorganic and Coordination Compounds*, 5th ed.; Wiley: New York, 1997; Part A, Section II.

(35) Jenkins, H. D. B.; Pratt, K. F. *Inorg. Chim. Acta* **1979**, *32*, 25.

that the metal-dependent bonding of a monoatomic adsorbate to an electrode surface shares some features with that of the same or similar ligands bound to a single metal atom. Unfortunately, however, there is a paucity of contemporary theoretical work concerned with interrelating the nature of bonding on metal surfaces and in simple inorganic complexes, especially with regard to the latter class of systems.

Having arrived at the above satisfyingly straightforward picture of periodic trends in electrochemical bonding of monoatomic species, one is tempted to examine diatomic adsorbates in the same fashion, especially the archetypical such chemisorbate, carbon monoxide. It is well-documented, however, that the metal-dependent intramolecular stretching frequencies (ν_{CO}) for chemisorbed CO do not correlate with d-band occupancy or related parameters.³⁶ This is due to the variable involvement of π -back-donation as well as σ -donation, along with the presence of different coordination geometries.^{20,30} Nonetheless, given the availability of metal–CO stretching ($\nu_{\text{M–CO}}$) as well as ν_{CO} SERS data on the Pt-group electrode surfaces of concern here,^{8,37} it is of interest to briefly examine the periodic trends. Unusually, the $\nu_{\text{M–CO}}$ frequencies are found to blueshift toward lower electrode potentials, a manifestation of enhanced π bonding at more negative electrode charges.^{37,39b} Although palladium engenders near-exclusive bridging coordination, with a characteristically lower $\nu_{\text{M–CO}}$ value (ca. 370 cm^{-1}), atop binding is nonetheless discernible from a weak ca. 450 cm^{-1} feature (at 0 V vs SCE).³⁷ More dominant atop $\nu_{\text{M–CO}}$ vibrations

are evident on platinum, rhodium, and iridium, with $\nu_{\text{M–CO}}$ values of 475, 445, and 515 cm^{-1} , respectively (also at 0 V vs SCE). The resulting $\nu_{\text{M–CO}}$ sequence, Rh \sim Pd < Pt < Ir, bears a resemblance to the monoatomic adsorbate periodic trends noted above, including the blueshifted frequencies of 5d versus 4d metals, with the highest metal–adsorbate frequency again being found on iridium. This implied stronger bonding for molecular as well as monoatomic adsorbates on Ir versus Pt is consistent with some theoretical predictions.³⁸

Overall, then, the present periodic trends seen for late transition metal and noble-metal bonding at electrochemical interfaces as discerned by SERS display a satisfying harmony with the available theoretical predictions, along with a broad consistency with the available experimental data for metal–vacuum systems. Given this situation, it would be desirable not only to examine metal–adsorbate vibrations for a wider range of metal electrodes and chemisorbates, but also to pursue in systematic fashion comparisons with contemporary ab initio theoretical calculations applied to charged as well as uncharged metal surfaces.^{22,39}

Acknowledgment. Dr. Shouzhong Zou provided valuable experimental advice. This work is supported by the National Science Foundation and the Petroleum Research Fund.

JA992640B

(36) For example, see: Masel, R. I. *Principles of Adsorption and Reaction on Solid Surfaces*; Wiley: New York, 1996; Chapter 3.10.

(37) Zou, S.; Weaver, M. J. *J. Phys. Chem.* **1996**, *100*, 4237.

(38) Reference 32a, p 117.

(39) (a) Koper, M. T. M.; van Santen, R. A. *Surf. Sci.* **1999**, *422*, 118.
(b) Koper, M. T. M.; van Santen, R. A. *J. Electroanal. Chem.* **1999**, *476*, 64.